

Dynamics of a biochemical system with multiple oscillatory domains as a clue for multiple modes of neuronal oscillations

A. Goldbeter and F. Moran*

Faculté des Sciences, Université Libre de Bruxelles, Campus Plaine, C.P. 231, B-1050 Brussels, Belgium

Received January 15, 1987/Accepted June 17, 1987

Abstract. We analyze the behavior of a two-variable biochemical model in conditions where it admits multiple oscillatory domains in parameter space. The model represents an autocatalytic enzyme reaction with input of substrate both from a constant source and from non-linear recycling of product into substrate. This system was previously studied for birhythmicity, i.e. the coexistence between two stable periodic regimes (Moran and Goldbeter 1984), and for multi-threshold excitability (Moran and Goldbeter 1985). When two distinct oscillatory domains obtain as a function of the substrate injection rate, the system is capable of exhibiting two markedly different modes of oscillations for slightly different values of this control parameter. Phase plane analysis shows how the multiplicity of oscillatory domains depends on the parameters that govern the underlying biochemical mechanism of product recycling. We analyze the response of the model to various kinds of transient perturbations and to periodic changes in the substrate input that bring the system through the two ranges of oscillatory behavior. The results provide a qualitative explanation for experimental observations (Jahnsen and Llinas 1984b) related to the occurrence of two different modes of oscillations in thalamic neurones.

Key words: Oscillations, biochemical model, thalamic neurones

1. Introduction

A conspicuous property of sustained oscillations in chemical and biological systems is that they only arise in well-defined conditions, corresponding to a particular domain in parameter space (Nicolis and Prigogine 1977; Winfree 1980). In experimental systems and in models as well, sustained oscillations generally occur

beyond a critical value of some control parameter or in a range bounded by two such critical values. The question arises as to what are the consequences of a multiplicity of oscillatory domains on the dynamics of systems capable of periodic behavior. Such multiplicity obtains whenever oscillations occur in two, or more, distinct ranges of values of a control parameter. As shown below, this situation may account for unexpected, or even paradoxical, modes of dynamic behavior.

Two-variable systems are particularly suited for analyzing the dynamic phenomena associated with multiple domains of periodic behavior, since these systems are amenable to phase plane analysis (Minorsky 1967). Here, we analyze a two-variable biochemical model presenting such multiplicity. The model is closely related to those previously proposed for the best-known examples of metabolic oscillations (see Goldbeter 1980; Goldbeter et al. 1984, for review), namely, glycolytic oscillations in yeast and muscle (Hess and Boiteux 1968; Frenkel 1968), and the periodic synthesis of cyclic AMP in the slime mold *Dicystelium discoideum* (Gerisch and Wick 1975).

By means of phase plane analysis, we show how multiple oscillatory domains originate from the underlying biochemical mechanism, and determine how this multiplicity influences the response of the system to transient or periodic changes in parameter values. Despite the biochemical nature of the mechanism considered, the results have immediate relevance to neurophysiology. The dynamic properties of the model indeed provide a qualitative explanation for recent findings on the existence of two distinct modes of oscillatory behavior in thalamic neurones.

2. Model and phase plane analysis

The model considered is that of an allosteric enzyme activated by its reaction product (Fig. 1). Such a model

* Present address: Department of Biochemistry, Faculty of Chemistry, Universidad Complutense, E-28040 Madrid, Spain

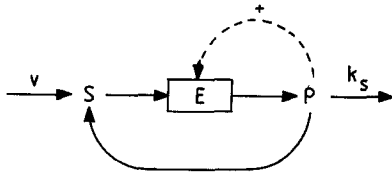


Fig. 1. Model of a product-activated enzyme reaction with recycling of product into substrate. This model, previously analyzed for birhythmicity and multi-threshold excitability (Moran and Goldbeter 1984, 1985), admits one or two oscillatory domains as a function of the substrate input v

has been analyzed extensively (Goldbeter and Nicolis 1976) in relation with glycolytic oscillations that occur in yeast and muscle, with a period of several minutes, as a result of the activation of phosphofructokinase by a reaction product (Frenkel 1968; Hess and Boiteux 1971; Goldbeter and Caplan 1976). Oscillations occur in the model when the constant substrate injection rate is in a range bounded by two critical values of the substrate input. This result agrees with the observation that glycolytic oscillations occur in yeast extracts when the substrate input lies between 20 and 160 mM/h; outside this range, the system evolves toward a stable steady state (Hess and Boiteux 1968).

Multiple oscillatory domains can arise in the model of Fig. 1 when product recycling into the substrate is taken into account (although such recycling also occurs in glycolysis where ADP is transformed into ATP, there is as yet no evidence for multiple ranges of substrate input producing glycolytic oscillations in yeast or muscle). Previous analyses of the model of Fig. 1 (Moran and Goldbeter 1984, 1985) have shown that product recycling may give rise, for a given set of parameter values, to birhythmicity (i.e., the coexistence of two simultaneously stable periodic regimes) and excitability with multiple thresholds (the latter property refers to the capability of the system to amplify in a pulsatory manner perturbations beyond two distinct thresholds for excitation). Both phenomena are closely associated with the existence of multiple oscillatory domains in parameter space.

The model comprises two variables, namely, the substrate and product concentrations, whose time evolution is governed by the kinetic equations (Moran and Goldbeter 1984):

$$\begin{aligned} \frac{d\alpha}{dt} &= v + \frac{\sigma_i \gamma^n}{K^n + \gamma^n} - \sigma_M \phi(\alpha, \gamma) \\ \frac{d\gamma}{dt} &= q \sigma_M \phi(\alpha, \gamma) - k_s \gamma - \frac{q \sigma_i \gamma^n}{K^n + \gamma^n} \end{aligned} \quad (1)$$

with

$$\phi(\alpha, \gamma) = \frac{\alpha(1+\alpha)(1+\gamma)^2}{L + (1+\alpha)^2(1+\gamma)^2}.$$

In the above equations, α and γ denote the normalized concentrations of substrate and product; v and σ_M denote the normalized input of substrate and maximum rate of the product-activated enzyme reaction; q is the ratio of the Michaelian constant of this enzyme, divided by the dissociation constant of the product; L is the allosteric constant of the product-activated enzyme; σ_i and K refer to the normalized maximum rate of product recycling and to the product concentration yielding the half-maximum rate of this process; k_s is the apparent first-order rate constant for removal of the product. Equations (1) are obtained by means of a quasi-steady-state hypothesis for all enzymatic forms, when assuming that the product-activated enzyme obeys the concerted model for allosteric enzymes (Monod et al. 1965), whereas the recycling process is governed by the Hill equation with a cooperativity coefficient n .

In the phase plane, the characteristics of the nullclines of system (1) determine the modes of dynamic behavior. The substrate and product nullclines obey Eqs. (2a) and (2b), respectively:

$$v = \sigma_M \phi(\alpha, \gamma) - \frac{\sigma_i \gamma^n}{K^n + \gamma^n} \quad (2a)$$

$$k_s \gamma = q \left[\sigma_M \phi(\alpha, \gamma) - \frac{\sigma_i \gamma^n}{K^n + \gamma^n} \right]. \quad (2b)$$

These relations are obtained from Eqs. (1) by setting $d\alpha/dt$ and $d\gamma/dt$ equal to zero. Whereas the product nullcline possesses but a single region of negative slope $d\alpha/d\gamma$ when $\sigma_i = 0$ (Fig. 2a), it can possess up to two such regions in the presence of product recycling (Fig. 2b). As in the case $\sigma_i = 0$ (Goldbeter 1980), linear stability analysis shows that the steady state, which lies at the intersection of the two nullclines, is unstable whenever the slope $d\alpha/d\gamma$ on the product nullcline is sufficiently negative and obeys inequality (3):

$$(d\alpha/d\gamma)_0 < -(1/q). \quad (3)$$

The system governed by Eqs. (1) admits a single steady state and remains bounded. Consequently, the instability of the steady state is associated with the evolution toward a stable limit cycle corresponding to sustained oscillations of α and γ as a function of time. A typical limit cycle is shown in Fig. 2a for $\sigma_i = 0$. In the presence of product recycling, limit cycles have a more complex structure that is analyzed in Sect. 4 below.

3. Origin of multiple oscillatory domains

In the absence of recycling, the product nullcline possesses only one region of negative slope in which condition (3) may hold. Thus, a single domain of oscillations obtains in these conditions, when varying the

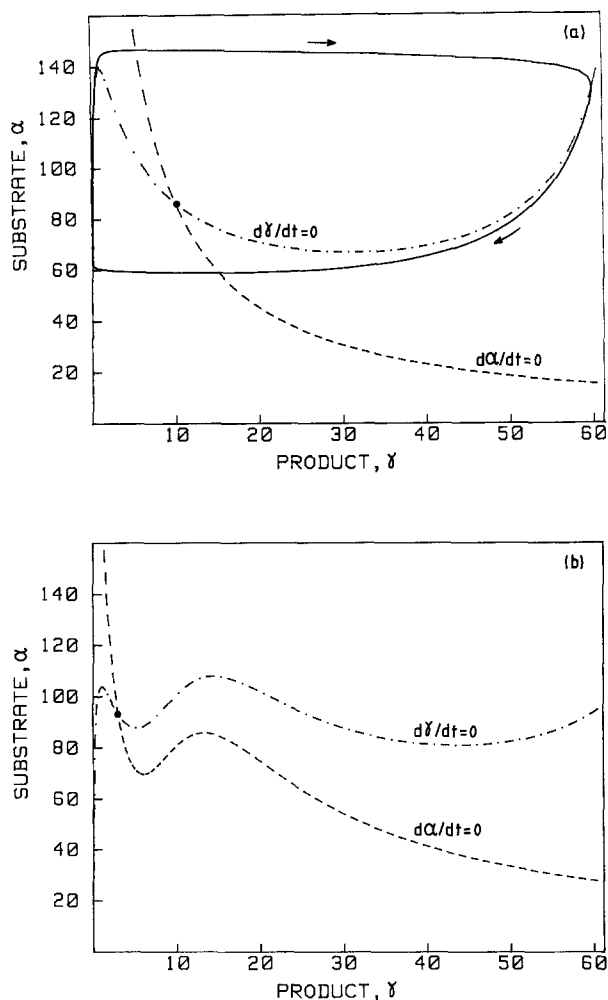


Fig. 2a and b. Substrate and product nullclines in the absence (a) or presence (b) of product recycling. The nullclines are given by Eqs. (2a, b). In (a) the product nullcline possesses but a single region of negative slope $d\alpha/d\gamma$, whereas two such regions exist in (b). The steady state, located at the intersection of the two nullclines, is unstable whenever the slope $d\alpha/d\gamma$ in this state is sufficiently negative. The solid curve in (a) shows the limit cycle that encloses such an unstable steady state in the phase plane (α, γ). The product nullcline is the locus of the steady state as a function of v (see text)

ratio (qv/k_s). This ratio will be taken here as bifurcation parameter since at steady state it is equal to the product concentration γ_0 . An increase in the substrate input v , which is the control parameter used in the experiments on glycolytic oscillations (Hess and Boiteux 1968), has the effect of shifting the substrate nullcline to the right without affecting the nullcline for γ . For a given ratio (q/k_s), the product nullcline therefore represents the locus of steady states when varying the substrate input, since the steady state is the intersection of this curve with the substrate nullcline that moves to the right upon increasing v .

Figures 3 and 4 indicate how product recycling leads to the emergence of two domains of instability separated by a range of parameter values for which the

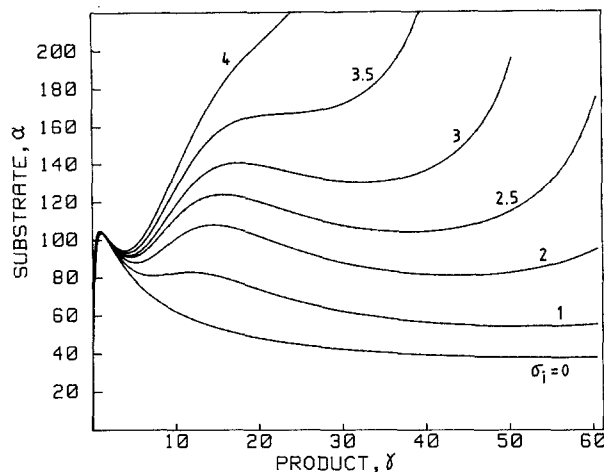


Fig. 3. Deformation of the product nullcline as a function of the maximum rate of product recycling. The curves show the product nullcline (Eq. 2b) for different values of the normalized, maximum recycling rate σ_i . Values of σ_i (in s^{-1}) are indicated on each curve. Other parameter values are: $q = 20$, $\sigma_M = 5.8 s^{-1}$, $n = 4$, $K = 12$, $L = 5 \cdot 10^6$, $k_s = 1 s^{-1}$

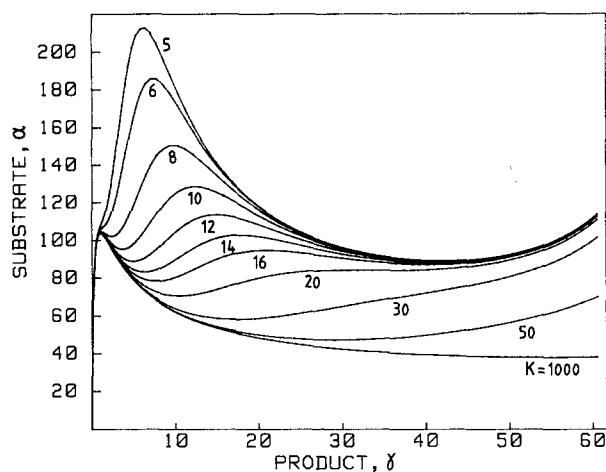


Fig. 4. Deformation of the product nullcline as a function of the threshold constant for product recycling. The curves are established according to Eq. (2b) for the parameter values of Fig. 3, with $\sigma_i = 2.2 s^{-1}$. The value of parameter K is indicated on each curve

steady state is stable. Two parameters govern the recycling process, namely, the maximum rate of recycling, σ_i , and the threshold constant K which yields a measure of the concentration γ at which recycling into α becomes significant.

In Fig. 3, the effect of increasing σ_i at the fixed value $K = 12$ appears to induce a "bump" in the product nullcline around the value $\gamma = K$. The form of the nullcline can be comprehended in terms of the steady state dependence of α and γ on v . In the absence of recycling, the value of α at steady state first increases with v , then begins to decrease as autocatalysis becomes significant when the product concentration, equal to (qv/k_s) at steady state, reaches a level close to unity. The reason for the decrease in the steady state

value of α upon increasing v is the enhanced rate of substrate consumption once autocatalysis becomes effective. The substrate concentration eventually rises again at larger values of v . This occurs because the enzyme is then fully activated by the high concentration of product: the enzyme reaction rate cannot increase further, so that substrate consumption is superseded by the substrate input.

Product recycling has the effect of counterbalancing the decrease in α brought about by autocatalysis. Indeed, provided the threshold constant K is in an appropriate range (see Fig. 4), any increase in γ beyond K will tend to increase the substrate level through the recycling reaction. This effect becomes more pronounced as the maximum rate of recycling increases. Hence, the "bump" produced around $\gamma = K$ becomes more pronounced as σ_i increases.

When the value of K is such that it corresponds to a value of γ located in the region of negative slope, the bump will create around $\gamma = K$ a region of stability as soon as condition (3) ceases to hold. At first, the original domain of instability still exists at larger values of γ , since the slope $d\alpha/d\gamma$ there remains sufficiently negative. However, when σ_i becomes larger than 3 s^{-1} in the case of Fig. 3, the second region of instability disappears altogether and only one domain subsists in which an unstable steady state is surrounded by a stable limit cycle.

The importance of the threshold constant for recycling is illustrated in Fig. 4 at a fixed value of σ_i . When the value of K is much larger than unity (e.g. $K = 1,000$), the product nullcline is nearly identical to that obtained with $\sigma_i = 0$. Indeed, as $\gamma \ll K$ in the range of product concentrations considered in Fig. 4, such a large value of K reduces the apparent rate of recycling to a negligible value.

A progressive decrease in K down to the value of 20 is seen to lead to an increase in the value of the slope $d\alpha/d\gamma$; this increase in slope occurs at lower and lower values of γ , so that the original instability domain shrinks upon decreasing K . Around $K = 15$, however, the effect of product recycling has moved sufficiently to the left, so that a region of negative slope reappears at larger values of γ : two domains of instability coexist. Further decrease in K leads to a progressive widening of the second instability domain and to a disappearance of the first, until the system once again admits a single oscillatory domain.

Figures 3 and 4 thus indicate that two domains of instability coexist as a function of the bifurcation parameter (qv/k_s) only in a finite range of values of the recycling parameters σ_i and K .

A third parameter related to product recycling is also determinant for the occurrence of multiple oscillatory domains. This is parameter n which measures the cooperative character of the recycling process. In-

deed, for two regions of negative slope to occur, the product nullcline has to correspond to a polynomial equation which is at least of the fifth degree in γ . This cannot occur for $n = 1$ since the product nullcline, which obeys Eq. (2b), is then of the third degree in γ . The nullcline equation has a degree equal to or greater than 5 only for $n \geq 2$. Numerical simulations indicate so far that multiple oscillatory domains, birhythmicity, and multi-threshold excitability occur in the model for $n \geq 3$.

4. Changing the time scale structure of the system changes the number of oscillatory domains

The existence of two separated domains of instability does not necessarily correspond to two distinct domains of oscillations. As shown by the series of bifurcation diagrams of Fig. 5, the existence of two separated domains of oscillations also depends on the time scale structure of the oscillatory system.

The diagrams of Fig. 5 were established for a moderate value of σ_i for which two regions of instability of

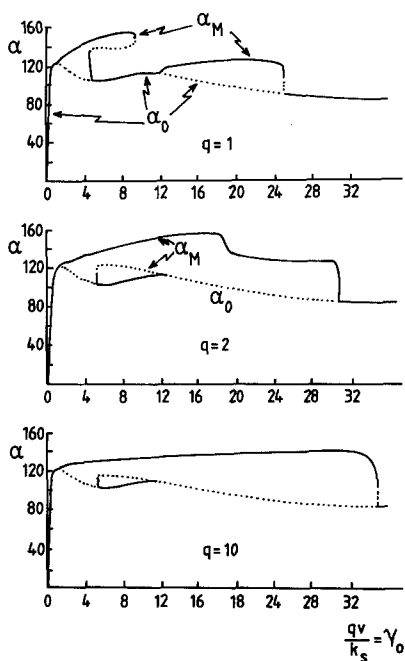


Fig. 5. Bifurcation diagram for three values of parameter q which governs the time scale structure of the system. In each graph, the steady state concentration of substrate, α_0 (lower curve), and the maximum substrate concentration in the course of oscillations, α_M (upper curves), are plotted as a function of v for fixed values of the ratio q/k_s . The abscissa yields the steady state concentration of product equal to qv/k_s . Solid and dotted lines refer, respectively, to stable and unstable (steady or periodic) regimes. The curves are established by combination of linear stability analysis and numerical integration of Eqs. (1). Parameter values are: $\sigma_i = 1.1 \text{ s}^{-1}$, $\sigma_M = 5 \text{ s}^{-1}$, $n = 4$, $K = 10$, $L = 5 \cdot 10^6$, $k_s = 0.06 q \text{ s}^{-1}$.

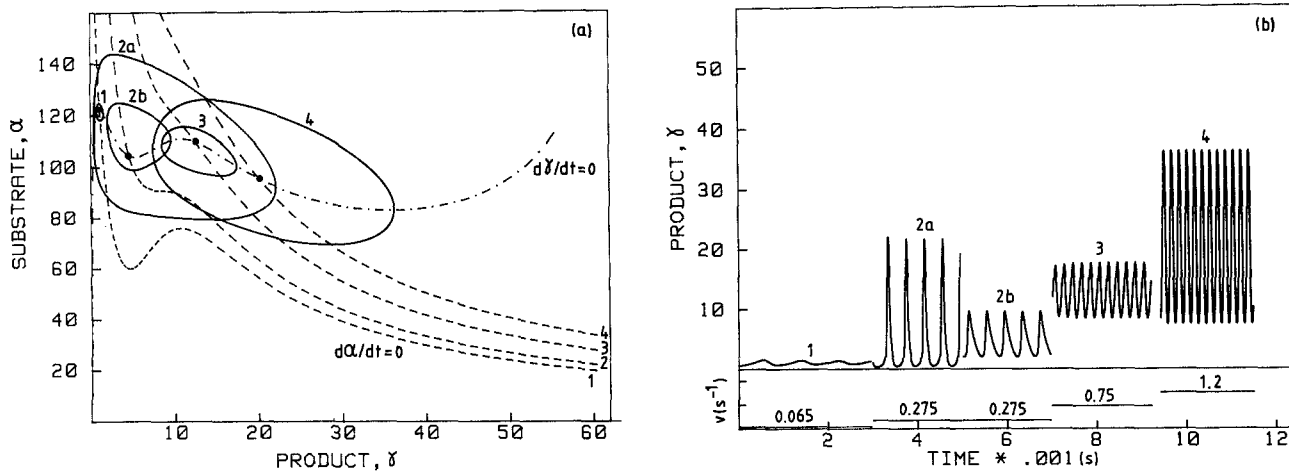


Fig. 6a and b. Limit cycle oscillations as a function of v for $q = 1$. The trajectories in the phase plane (a) and the time evolution (b) are shown for $v = 0.065 \text{ s}^{-1}$ (1), 0.275 s^{-1} (2), 0.75 s^{-1} (3) and 1.2 s^{-1} (4). The product nullcline is shown in the phase plane, together with the substrate nullclines corresponding to the four values of v . Two stable limit cycles coexist for $v = 0.275 \text{ s}^{-1}$; these are separated by an unstable cycle (not shown). The trajectories are obtained by numerical integration of Eqs. (1), whereas the nullclines are generated according to Eqs. (2). Parameter values are those of Fig. 5a

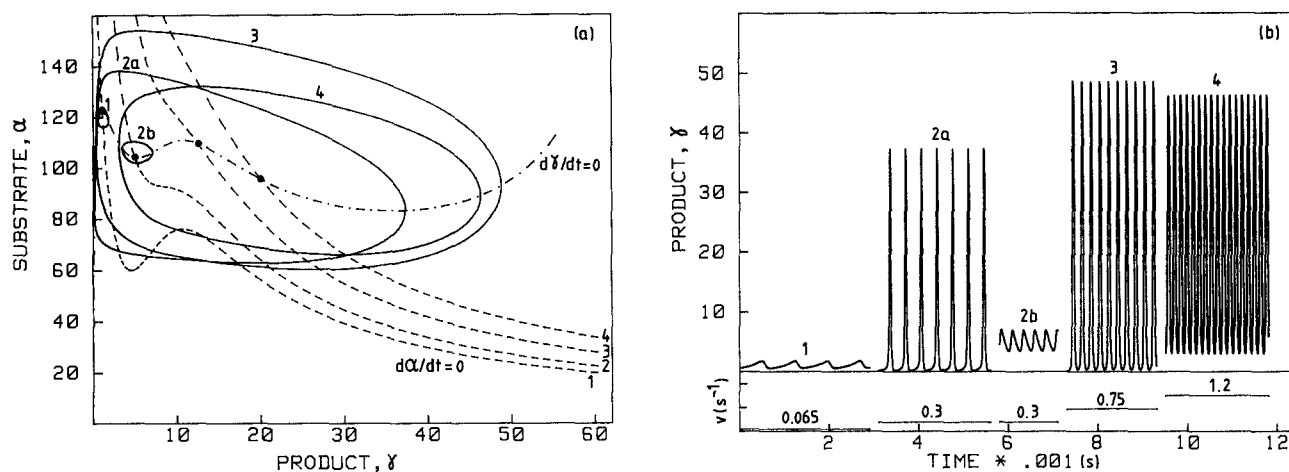


Fig. 7a and b. Limit cycle oscillations as a function of v for $q = 2$. The phase plane trajectories (a) and time evolution (b) are shown for four different values of the substrate input v (in s^{-1}): 0.065 (1), 0.3 (2), 0.75 (3), and 1.2 (4). Birhythmicity obtains here for $v = 0.3 \text{ s}^{-1}$. The curves are obtained as described in Fig. 6, for the parameter values of Fig. 5b

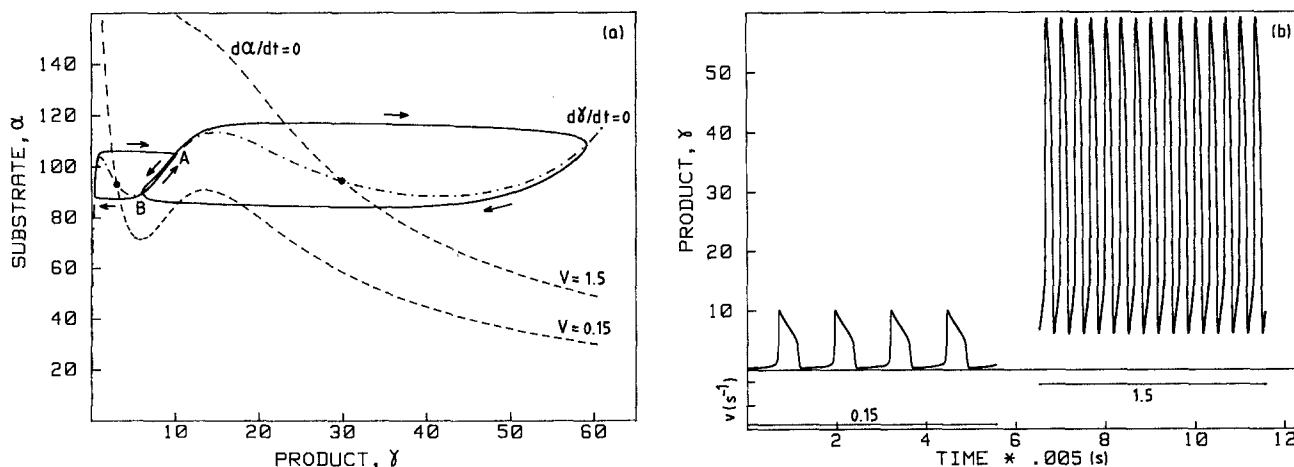


Fig. 8a and b. Two distinct types of oscillations predicted by the model for two values of the substrate input. The phase plane trajectories (a) and the corresponding time evolution (b) are shown for $v = 0.15 \text{ s}^{-1}$ and 1.5 s^{-1} . Due to the form of the product nullcline, these values produce, respectively, a small-amplitude and a large-amplitude limit cycle. The curves are obtained by numerical integration of Eqs. (1) for the parameter values of Fig. 3, with $\sigma_i = 2.2 \text{ s}^{-1}$. For $v = 0.9 \text{ s}^{-1}$, the large-amplitude limit cycle encloses the small-amplitude cycle (not shown; see also Fig. 7a)

the steady state are separated by a region of stability. Of importance here is the fact that the bump induced in the product nullcline by recycling, around the value $\gamma = K$, remains lower than the local maximum in this nullcline around $\gamma = 1$. Here we increase parameters q and k_s by a similar factor, in order not to affect the shape of the product nullcline nor the value of γ_0 which remains constant at a fixed value of v .

As shown by Eqs. (1), the rise in q and k_s enhances the rate of product evolution whereas the evolution rate of the substrate remains unchanged. The increase in the two parameters thus modifies the time scale structure of the system by making the product evolve faster than the substrate.

When product and substrate evolve on a similar time scale (see Fig. 5 for $q = 1$), the bifurcation diagram indicates two regions of oscillations separated by a range of v values corresponding to a stable steady state. Two additional phenomena, previously studied in more detail (Moran and Goldbeter 1984, 1985), are illustrated by this diagram, namely, birhythmicity and hard excitation. These refer, respectively, to the coexistence between two stable periodic regimes or between one stable steady state and one periodic regime, at a given value of the bifurcation parameter (qv/k_s). Upon increasing q and k_s , these two phenomena subsist but, due to the faster evolution of variable γ , the phase plane trajectories "jump over" the bump so that the two branches of periodic solutions merge. A continuous oscillatory domain obtains in these conditions as a function of (qv/k_s).

How the shape of the oscillations is affected by the existence of one or two time scales is further illustrated in Figs. 6 and 7, respectively. Here, four different input rates of substrate are considered. In Fig. 6, owing to the presence of two distinct oscillatory domains, the amplitude of the oscillations passes through a maximum and then increases again upon increasing v . This does not occur in Fig. 7, where there is a single oscillatory domain. In the latter case, the limit cycle obtained for $v = 0.75 \text{ s}^{-1}$ encloses that obtained for the larger value $v = 1.2 \text{ s}^{-1}$, whereas the reverse is true when the system admits a single time scale (compare also the bottom panels of Figs. 6 and 7). Birhythmicity obtains in both cases: depending on initial conditions, the system then evolves to either one of two stable periodic regimes.

The differential effect of one versus two time scales on the structure of the oscillatory domains markedly depends on the shape of the product nullcline. When the bump created by recycling surpasses the first maximum on this nullcline at larger values of σ_i , two well separated domains of oscillations are observed regardless of the time scale structure of the system. These oscillations are strikingly different, as shown in Fig. 8 where the limit cycles obtained for $v = 0.15 \text{ s}^{-1}$ and

1.5 s^{-1} are represented. A peculiar feature of these two cycles is that they share a portion of their trajectories. This common portion, denoted AB, is travelled from A to B on the small cycle, but in the reverse direction on the larger cycle.

5. Response to square-pulse or periodic perturbations

The above phase plane analysis permits one to predict the response of the oscillatory system to transient changes in the controlling parameters. Of particular interest is the response to square-wave pulses in the substrate injection v . Such pulses can indeed be compared to those used in neurophysiological experiments (see Discussion below).

Illustrated in Fig. 9a is a situation in which four different values of v are considered. These correspond to four different steady states (heavy dots), numbered from 1 to 4; only steady state 4 is unstable. In Fig. 9b, starting from the first steady state for $v = 0.05 \text{ s}^{-1}$, we impose a square pulse during which v is raised to 0.3 s^{-1} ; the system switches to steady state 2 after a small overshoot in γ , before returning to the original steady state. The input v is then raised transiently to 0.6 s^{-1} , and the level of γ settles to the new steady state in a hyperbolic manner, before decreasing exponentially when the square pulse terminates. Finally, a step increase in v from 0.6 to 1.5 s^{-1} induces sustained oscillations which cease when v is returned to the former value. The successive increases in v applied over an increasing background thus produce three different types of transient response. These can readily be comprehended by referring to the phase plane dynamics depicted in Fig. 9a.

For the parameter values of Fig. 9, we now consider the intermediate value $v = 0.55 \text{ s}^{-1}$ corresponding to a stable, non-oscillatory state (Fig. 10). A square pulse decrease in v down to 0.15 s^{-1} will produce regular, small-amplitude oscillations. An opposite pulse of the same magnitude, bringing v up to 0.95 s^{-1} , produces another type of oscillations whose period and amplitude markedly differ from those obtained with the transient decrease in v .

A specific consequence of the nullcline structure of the model is the existence of an overshoot phenomenon, already noticeable in Fig. 9a for the transition from $v = 0.05$ to 0.3 s^{-1} . When the oscillations obtained for $v = 0.8 \text{ s}^{-1}$ are terminated upon lowering v down to 0.3 s^{-1} , the subsequent evolution toward a stable steady state follows the passage through a similar overshoot (Fig. 11). The origin of such behavior is the same in both cases. For $v = 0.8 \text{ s}^{-1}$, the oscillations have the largest amplitude and the limit cycle goes all the way to the left limb of the product nullcline (see curve 3 established for $v = 0.75 \text{ s}^{-1}$ in Fig. 7a).

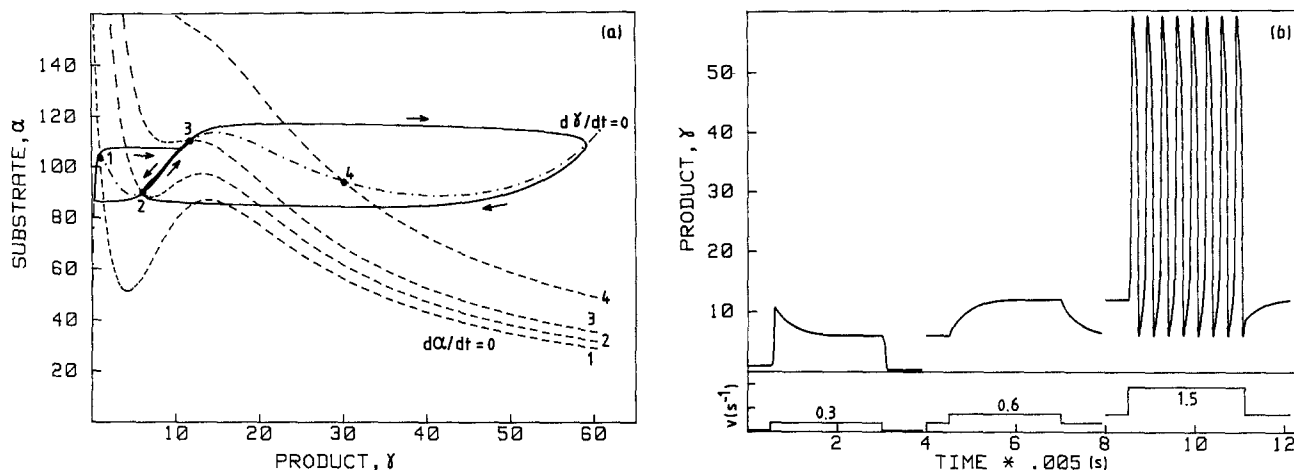


Fig. 9a and b. Effect of successive increments in v on oscillatory behavior. Shown are the phase plane trajectories (a) and time evolution (b) in response to three square-pulse increases in v (lower trace in panel b): 0.05 to 0.3, 0.3 to 0.6, and 0.6 to 1.5 (in s^{-1}). The first increment gives rise to an overshoot due to the presence of a central "bump" on the product nullcline. The second increment produces a monotonous evolution toward a stable steady state, whereas the third increase in v gives rise to sustained oscillations around an unstable steady state. In (a) the product nullcline is represented by a *dashed-dotted* line whereas the substrate nullclines numbered 1–4 which correspond to the values $v = 0.05, 0.3, 0.6, 1.5$ (in s^{-1}) are represented by *dashed* lines. The curves are established for the parameter values of Fig. 8

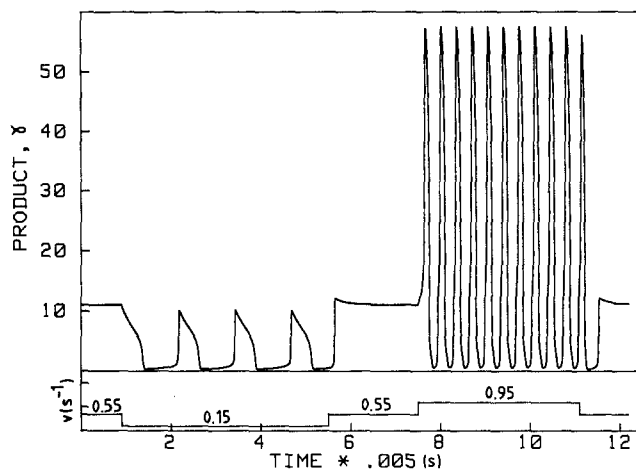


Fig. 10. Distinct modes of oscillatory behavior observed upon increasing or decreasing v with respect to a value of the substrate input yielding a stable steady state. Parameter v (lower trace) is first decreased from 0.55 to 0.15 s^{-1} , brought back to the initial value, and then raised to 0.95 s^{-1} . The curve is obtained by integration of Eqs. (1) for the parameter values of Fig. 8

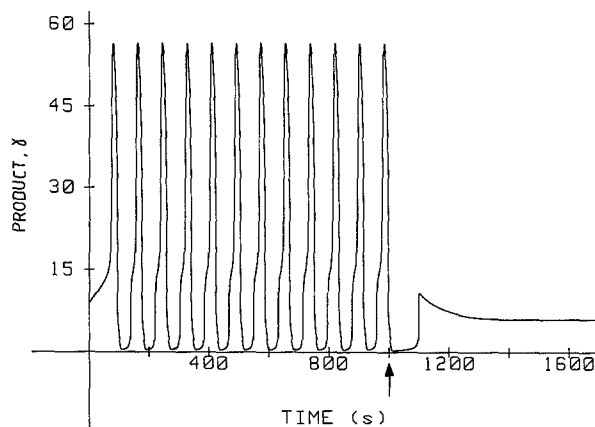


Fig. 11. Rebound excitation observed upon terminating oscillations by reducing the substrate input v from 0.8 to 0.3 s^{-1} in $t = 1,000$ s (arrow). The origin of the overshoot phenomenon that precedes the evolution toward the stable steady state is due, as in Fig. 9, to the fact that the second maximum on the product nullcline is higher than the first. Parameter values are as in Fig. 8

When the input rate is switched to 0.3 s^{-1} , the new steady state which lies in the first well on the nullcline is reached only after the trajectory hits the second region of positive slope on this nullcline. After the product concentration has reached this value, which corresponds to the maximum of the overshoot, it decreases as the trajectory brings the system to the stable steady state. The existence of the overshoot closely depends on the initial and final values of the controlling parameter, namely, the substrate input. Thus, no

overshoot would be observed if parameter v were decreased from 0.8 to 0.6 s^{-1} (see Fig. 9a).

In Fig. 12 is shown the response of the system to a positive, periodic variation in v . When the amplitude of the change is such that the maximum value of v corresponds to a stable steady state and the intermediate values produce large-amplitude oscillations, a characteristic response is obtained in which a series of spikes in γ occur both during the ascending and the descending ramps; these bursts are separated by a

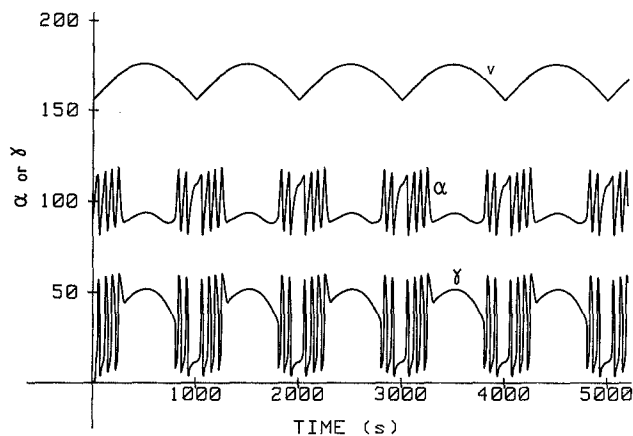


Fig. 12. Modulation of oscillatory behavior by a positive periodic variation in v . The substrate input is varied from 0.6 to 2.6 s^{-1} (upper trace, not scaled) according to the relation $v = 0.6 + 2|\sin(2\pi t/2,000)|$. Parameter values are those of Fig. 8

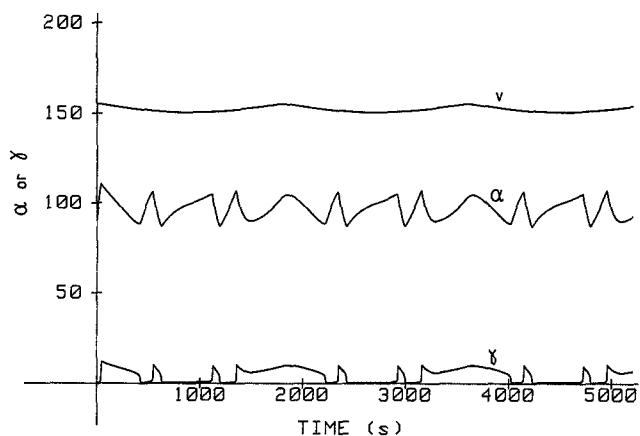


Fig. 13. Modulation of oscillatory behavior by a negative periodic variation in v . Parameter v varies from 0.05 to 0.55 s^{-1} according to the relation $v = 0.55 - 0.5|\sin(2\pi t/4,000)|$. Parameter values are as in Fig. 8

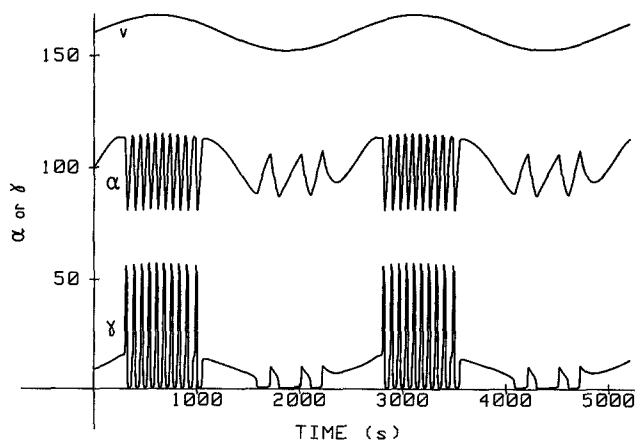


Fig. 14. Periodic forcing through multiple oscillatory domains. The substrate input (upper trace, not scaled) is varied from 0.11 to 0.91 s^{-1} according to the relation $v = 0.51 + 0.4 \sin(2\pi t/2,500)$. The curves are obtained by numerical integration of Eqs. (1) for the parameter values of Fig. 8

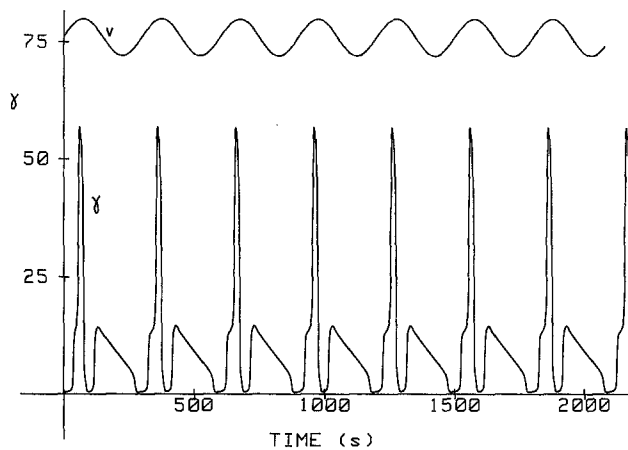


Fig. 15. Effect of a periodic variation in v similar to that in Fig. 14, with a period of 300 s instead of 2,500 s. Only the time evolution of the reaction product is shown

phase of quiescence around the maximum in v . The number of spikes on both sides increases with the period of the variation in v . For lower values of v , the second type of oscillation would also be observed.

A mirror variation in the substrate input give rise to a similar effect (Fig. 13), but the quiescent phase separates here small-amplitude bursts in γ ; these bursts are of the same type as those associated with oscillations at low values of the substrate input (see, e.g., Fig. 8 b).

Both types of oscillations can be seen to alternate periodically when the substrate input is varied in a sinusoidal manner such that v passes through the two oscillatory domains. Thus, in Fig. 14, v oscillates from 0.11 to 0.91 s^{-1} , around the mean value 0.51 s^{-1} , with a period of 2,500 s. Over such a period, a series of high-frequency bursts in γ occur with a large amplitude when v is above the mean; these precede a few low-amplitude peaks which are produced when v goes to its minimum. The effect of a periodic variation in v around the same mean value, but with a much shorter period (i.e. 300 s), is shown in Fig. 15. Here, each oscillatory domain is swept across so rapidly that a single high-amplitude spike in γ alternates with a single low-amplitude peak.

Whereas large-amplitude variations in substrate input produce the periodic patterns of Figs. 12–15, the sinusoidal modulation of parameter v , when restricted in a much smaller domain of variation, may produce quasi-periodic behavior. In the region of birhythmicity, the two coexisting limit cycles transform into two coexisting tori when a small sinusoidal variation is added to the substrate input v . We are currently investigating the conditions in which periodic forcing induces aperiodic oscillations, i.e. chaos, in this model.

6. Discussion

We have analyzed in a simple biochemical model the various oscillatory phenomena that arise in the presence of multiple oscillatory domains. Such domains occur as a function of a given parameter when two (or more) distinct oscillatory regimes, separated by a region of non-oscillatory behavior, obtain upon continuous variation of this parameter. The occurrence of multiple oscillatory domains in the two-variable model considered was readily explained in terms of the underlying biochemical mechanism by phase plane analysis.

Of primary importance for such multiplicity is the existence of a nullcline with two regions of negative slope corresponding to two domains of instability of the steady state. The relative positions of these two regions of negative slope, together with the time scale structure of the system, determine whether a single or two domains of oscillations will obtain.

The main result of the present analysis is to show how a given oscillatory system is capable of exhibiting two markedly different modes of periodic behavior in closely related conditions. The latter phenomenon differs from that of birhythmicity in which two modes of periodicity coexist in the same conditions. Here, however, the two phenomena are linked as birhythmicity occurs owing to the splitting of a single oscillatory domain into two parts (Moran and Goldbeter 1984). As shown by the present model, birhythmicity often occurs in a restricted domain of parameter values. The switching between two different periodic regimes in conditions of birhythmicity (Moran and Goldbeter 1984) should therefore be less common than that associated with the transition between multiple oscillatory domains in parameter space. With respect to physiological significance, a system oscillating with substantially different period and amplitude for slight changes in parameter values retains much of the versatility associated with birhythmic behavior.

No experimental example as yet exists for multiple oscillatory domains in enzymatic reactions. Beyond the dynamics of oscillatory biochemical systems the present results bear, however, on other biological rhythms, in particular those of neural origin.

Jahnsen and Llinas (1984a, b) have studied the neurophysiology of guinea pig thalamic neurones in vitro and showed that these cells are capable of exhibiting two different rhythms triggered at distinct membrane potential levels which differ by a few mV only. The first oscillation occurs at a level slightly depolarized from rest, with a frequency close to 10 Hz. The second oscillation occurs at more hyperpolarized levels, with a frequency close to 6 Hz. The physiological importance of such behavior stems from that these two frequencies coincide with the γ and θ rhythms of the

e.g. and, in the second case, with the frequency of Parkinson's tremor (Llinas 1984).

The various ionic conductances that underlie the two rhythmic processes have been analyzed in detail by Jahnsen and Llinas (1984 a, b). These authors relate the occurrence of two distinct oscillatory modes to the existence of both a low- and a large-threshold firing mechanism in thalamic neurones. Similar properties were also demonstrated in neurones of the inferior olive (Llinas and Yarom 1981, 1986). It is of interest that the present model may similarly possess the property of multi-threshold excitability: in the same conditions, the system then amplifies perturbations above two distinct thresholds before returning to the same stable steady state (Moran and Goldbeter 1985).

The present findings can be related to neuronal dynamics when taking the steady-state level of variable γ as a measure of the resting membrane potential. In such correspondence, a change in substrate input v leads to a change in the steady state level of product γ , and can therefore be associated with a change in applied current that shifts the resting potential. A transient increase or decrease in v then corresponds to a depolarizing or hyperpolarizing current pulse, respectively.

That the present model may prove useful for comprehending the oscillatory properties of thalamic neurones is further suggested by the striking resemblance of the results shown in Fig. 9 b with those presented in Fig. 2 of the paper by Jahnsen and Llinas (1984 a). There, a depolarizing pulse of fixed magnitude was given to thalamic cells, at three increasing values of the resting potential. For the most hyperpolarized state, the current pulse triggers an excitable response whereas for the medium value the same pulse only produces a subthreshold depolarization. For the most depolarized state the current pulse generates a train of action potentials.

Further similarities between the present results and the experiments on thalamic neurones relate to the effect of double-ramp current injection. The above simulations (see, e.g., Fig. 12) show that the dynamics of the biochemical system differs during the rising and decreasing phases of the input variation. The number of peaks in both phases is different, although the system traverses the same range of input values. Such "hysteresis" is also observed in the experiments (see Fig. 11 of Jahnsen and Llinas 1984 b).

Finally, the analysis of the model indicates the conditions in which a phenomenon of rebound excitation resembling that observed in thalamic cells (Jahnsen and Llinas 1984 a, b) is associated with the existence of two oscillatory domains. The occurrence of this phenomenon following a change in the substrate input depends on the final value of this parameter.

Biochemical oscillations result from the regulation of enzyme activity by non-linear feedback processes. Such regulations are often of an autocatalytic nature, as in the present model. Neuronal oscillations likewise originate from non-linear ionic transport processes which are frequently autocatalytic, through their voltage dependence.

Although there is no direct relation between the biochemical variables of this model and those governing the excitability of nerve cells, the above discussion shows that the present results account qualitatively for many oscillatory properties of thalamic neurones. This further supports our suggestion based on multi-threshold excitability (Moran and Goldbeter 1985) that a phase portrait similar to that furnished by the present model may underlie the dynamic behavior of thalamic cells.

The occurrence of multiple modes of thalamic oscillations can indeed be linked in the phase plane to the existence of a nullcline with two regions of negative slope. The fact that the variables here are biochemical instead of current and voltage in the neuronal system should not prevent relating the present results to thalamic behavior. From a dynamic point of view, the key issue is that similar dynamic phenomena are associated with similar phase portraits.

The above view is corroborated by a recent study of Rose and Hindmarsh (1985) who proposed a model for thalamic cells, on the basis of a nullcline structure similar to that of the present model. These authors indeed consider a two-variable model in which the nullcline for the membrane potential possesses two regions of negative slope; to this end, the equation for this nullcline is taken as a combination of two cubic polynomials. Rose and Hindmarsh show that such nullcline shape gives rise to two instability domains and use it to account for the multiple modes of oscillations observed in thalamic neurones, as well as for a variety of experimental results on the effect of current pulses.

Beyond the very nature of the variables considered, the main difference between this model and that of Rose and Hindmarsh is that the present one provides an explicit molecular mechanism giving rise to a nullcline with two regions of instability. The continuous deformation of the nullcline due to changes in the rate or in the threshold for product recycling leads to patterns of dynamic behavior which range from a unique periodic regime to birhythmicity and multiple modes of oscillations. In the model for thalamic neurones (Rose and Hindmarsh 1985), similar nullcline deformations assigned to changes in ionic currents produce, in a similar manner, increasingly complex patterns of rhythmic activity.

The adequacy of the present model for the qualitative description of some of the excitable and oscil-

latory properties of thalamic cells raises the possibility that birhythmicity may also occur in these neurones – as well as in the Rose-Hindmarsh model – in an appropriate range of the membrane potential. Our previous analysis shows, however, that birhythmicity obtains only in a limited range of values of the substrate input and of other parameters such as the maximum rate and the threshold constant for recycling (Moran and Goldbeter 1984). The model also suggests (see Figs. 14 and 15) that a sinusoidal variation of the applied current with the appropriate amplitude and frequency should produce a pattern of temporal response characterized by alternation between the two oscillatory modes of thalamic cells.

The interest of the present model for the study of phenomena associated with multiple oscillatory domains stems from its relative simplicity and from the fact that its nullcline structure can be readily modified by changes in the parameters that govern a well-defined molecular process, i.e. product recycling. Such versatility may be useful in addressing different types of experimental situations. With respect to modelling dynamic phenomena in neuronal systems, the present model may be viewed as providing an alternative to models based on Hodgkin-Huxley equations or on mathematical descriptions not directly related to underlying biophysical mechanisms.

Acknowledgements. We thank Dr. R. Llinas for stimulating discussions. One of the authors (F. M.) held a fellowship from the European Molecular Biology Organization (EMBO) during completion of this work.

References

- Frenkel R (1968) Control of reduced diphosphopyridine nucleotide oscillations in beef heart extracts. I. Effects of modifiers of phosphofructokinase activity. *Arch Biochem Biophys* 125:151–156
- Gerisch G, Wick U (1975) Intracellular oscillations and release of cyclic AMP from *Dictyostelium* cells. *Biochem Biophys Res Commun* 65:364–370
- Goldbeter A (1980) Models for oscillations and excitability in biochemical systems. In: Segel LA (ed) *Mathematical models in molecular and cellular biology*. Cambridge University Press, Cambridge, pp 248–291
- Goldbeter A, Caplan SR (1976) Oscillatory enzymes. *Annu Rev Biophys Bioeng* 5:449–476
- Goldbeter A, Nicolis G (1976) An allosteric enzyme model with positive feedback applied to glycolytic oscillations. In: Snell F, Rosen, R (eds) *Progress in theoretical biology*, vol 4. Academic Press, New York, pp 65–160
- Goldbeter A, Martiel JL, Decroly O (1984) From excitability and oscillations to birhythmicity and chaos in biochemical systems. In: Ricard J, Cornish-Bowden A (eds) *Dynamics of biochemical systems*. Plenum Press, New York, pp 173–212
- Hess B, Boiteux A (1968) Control of glycolysis. In: Järnefelt J (ed) *Regulatory functions of biological membranes*. Elsevier, Amsterdam, pp 148–162

- Hess B, Boiteux A (1971) Oscillatory phenomena in biochemistry. *Annu Rev Biochem* 40:237–258
- Jahnsen H, Llinas R (1984a) Electrophysiological properties of guinea-pig thalamic neurones: an in vitro study. *J Physiol* 349:205–226
- Jahnsen H, Llinas R (1984b) Ionic basis for the electroresponsiveness and oscillatory properties of guinea-pig thalamic neurones in vitro. *J Physiol* 349:229–247
- Llinas R (1984) Rebound excitation and the physiological basis for tremor: a biophysical study of the oscillatory properties of mammalian central neurones in vitro. In: Findley LJ, Capildeo R (eds) *Movement disorders: Tremor*. Macmillan, London, pp 165–182
- Llinas R, Yarom Y (1981) Properties and distribution of ionic conductances generating electroresponsiveness of mammalian inferior olivary neurones in vitro. *J Physiol* 315:569–684
- Llinas R, Yarom Y (1986) Oscillatory properties of guinea-pig inferior olivary neurones and their pharmacological modulation: an in vitro study. *J Physiol* 376:163–182
- Minorsky N (1967) *Nonlinear oscillations*. Van Nostrand, Princeton, NJ
- Monod J, Wyman J, Changeux JP (1965) On the nature of allosteric transitions: a plausible model. *J Mol Biol* 123:88–118
- Moran F, Goldbeter A (1984) Onset of birhythmicity in a regulated biochemical system. *Biophys Chem* 20:149–156
- Moran F, Goldbeter A (1985) Excitability with multiple thresholds: a new mode of dynamic behavior analyzed in a regulated biochemical system. *Biophys Chem* 23:71–77
- Nicolis G, Prigogine I (1977) *Self-organization in nonequilibrium systems*. John Wiley, New York
- Rose RM, Hindmarsh JL (1985) A model for a thalamic neuron. *Proc R Soc Lond B* 225:161–193
- Winfree AT (1980) *The geometry of biological time*. Springer, New York Berlin Heidelberg